

Supplementary Materials for  
**Chromatographic separation of active polymer-like worm mixtures by  
contour length and activity**

Tess Heeremans *et al.*

Corresponding author: Antoine Deblais, [a.deblais@uva.nl](mailto:a.deblais@uva.nl); Daniel Bonn, [d.bonn@uva.nl](mailto:d.bonn@uva.nl); Sander Woutersen,  
[s.woutersen@uva.nl](mailto:s.woutersen@uva.nl)

*Sci. Adv.* **8**, eabj7918 (2022)  
DOI: [10.1126/sciadv.abj7918](https://doi.org/10.1126/sciadv.abj7918)

**This PDF file includes:**

Figs. S1 to S6

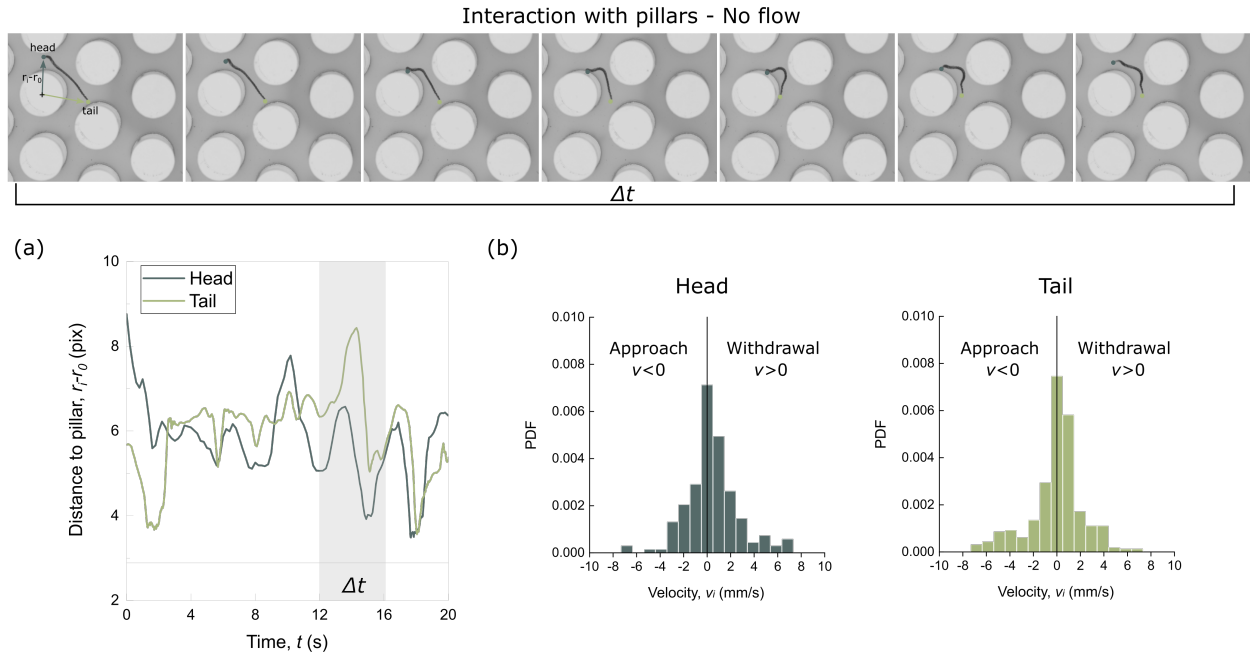


**FIG. S 1. Dynamics of worm-pillar collisions.** (a) Snapshot of the radial velocity component of the two endpoints of a *Tubifex* worm as a function of time. (b) Statistical distribution of the radial velocity of the endpoints.

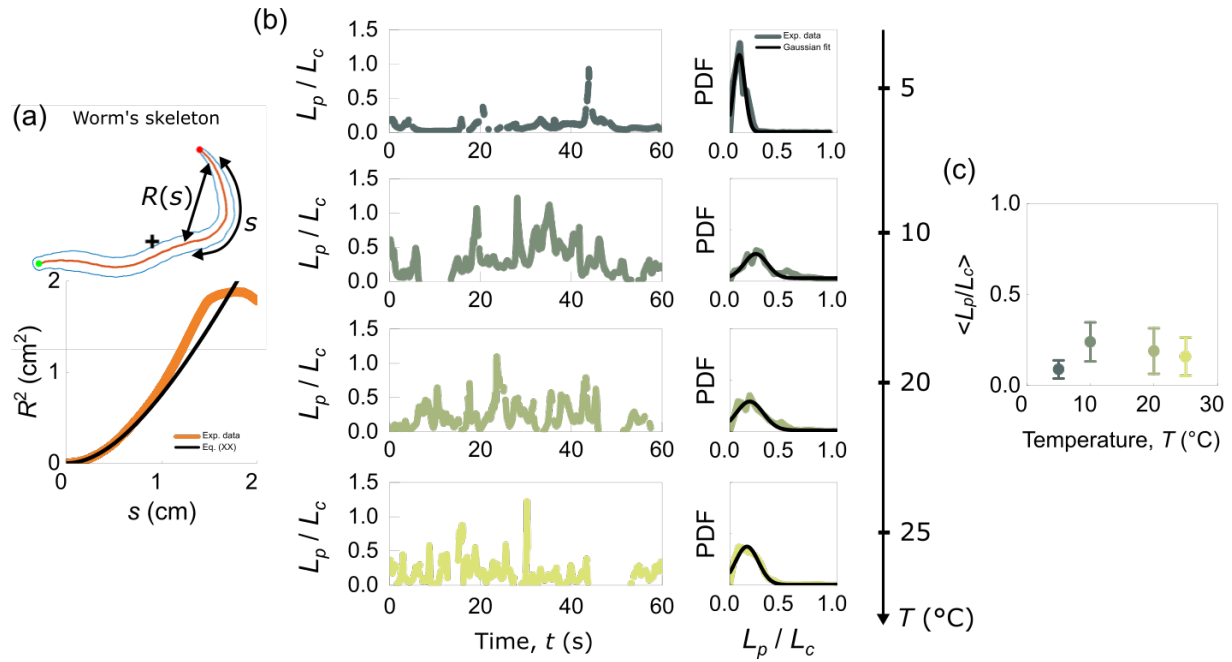


FIG. S 2. **Persistence length: effect of the temperature.** (a) The persistence length  $L_p$  of a worm at a given temperature  $T$  and time  $t$  is determined by fitting the dependence of the end-to-end distance  $R(s)$  with the contour length  $s$  (Eq. 1 in the main text). (b) The persistence length is reported over 60 s (normalized by the worm's contour length  $L_c$ ) for an overall of 3000 consecutive conformations (the worm's shape is followed in time at a frame rate of 50 frames per second). The corresponding probability function (PDF) is plotted for the different temperatures investigated (coloured line). From the latter, we extracted the averaged value of the persistence length (c) as a function of temperature by fitting a Gaussian distribution. Error bars are standard deviations.

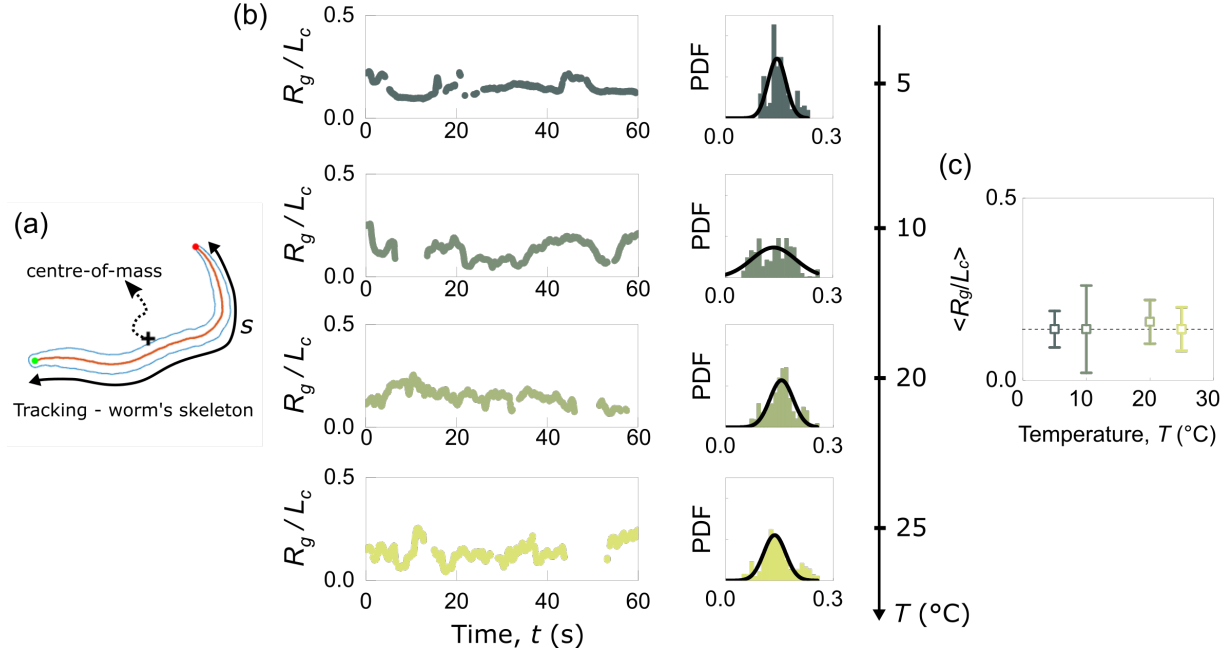


FIG. S 3. **Influence of activity (temperature) on worm's radius of gyration.** (a) The worm's skeleton (orange) is tracked from imaging and the radius of gyration is extracted from  $R_g^2 = \frac{1}{N} \sum_{i=1}^N (\vec{r}_i - \vec{r}_{com})^2$ . (b) Time-dependent radius of gyration normalized by the contour length at different temperatures, together with the corresponding probability distribution functions. (c) Average radius of gyration as a function of temperature.

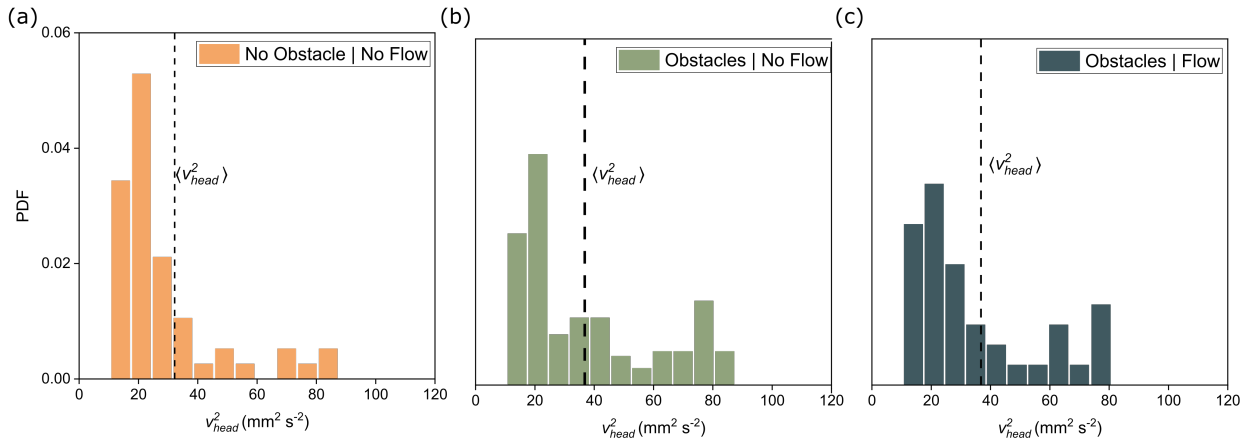


FIG. S 4. **Effect of the pillar array and flow current on the activity.** Shown are the distributions of the kinetic energy  $v(t)^2$  (where  $v(t)$  is the time-dependent velocity) of the worm's end point in three different circumstances: (a) free space (water tank, no flow); (b) in a pillar array in absence of flow; (c) in a pillar array in the presence of flow.

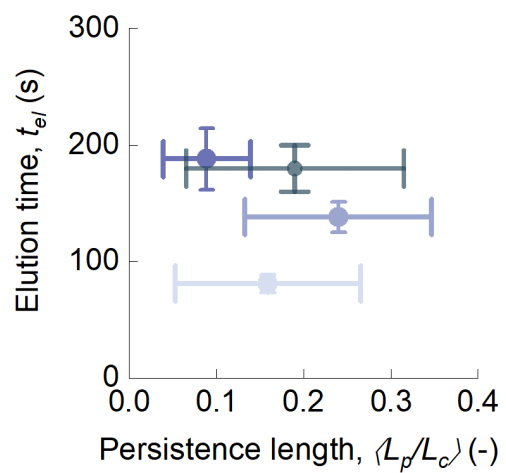
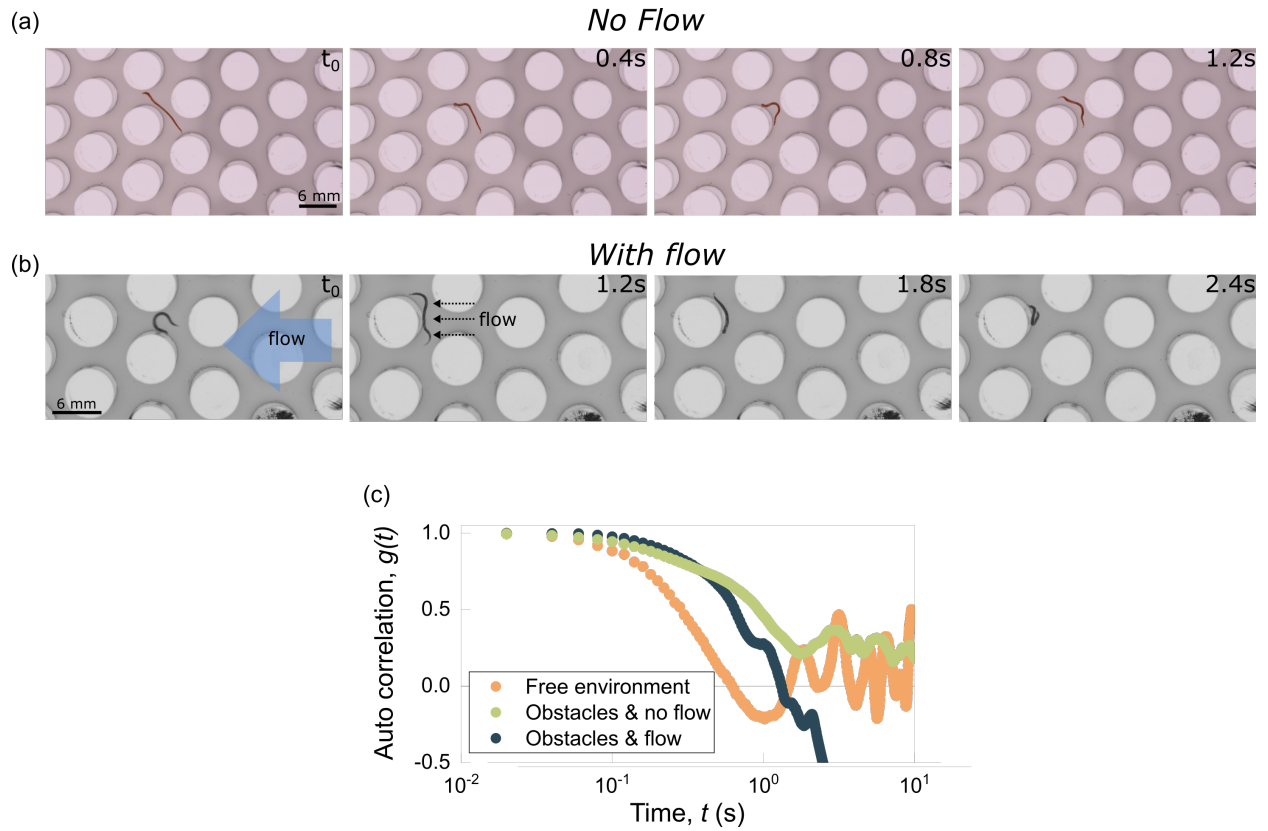


FIG. S 5. **Elution time vs. persistence length.** The elution times are reported as a function of the persistence length measured in Fig. S2. No correlation is observed.



**FIG. S 6. Influence of pillars and flow on worm's relaxation time.** An active worm ( $T = 20^\circ$ ) is placed in the post array without (a) and in the presence of a flow (b), and its shape's fluctuations are followed in time compared to the same worm when placed in a free environment (orange). Interaction with the pillars and with the flow induce significant temporal variation of the end-to-end distance than in a free environment, as indicated by the increase of the relaxation time extracted from the autocorrelation function (c).